

Parameterization of the Absorption of the H₂O Continuum, CO₂, O₂, and Other Trace Gases in the Fu-Liou Solar Radiation Program

ZHANG Feng*¹ (张 凤), ZENG Qingcun¹ (曾庆存), Y. GU², and K. N. LIOU²

¹*Institute of Atmospheric Physics, Chinese Academy of Sciences, Beijing 100029*

²*Department of Atmospheric and Oceanic Sciences, University of California Los Angeles, California 90095*

(Received 2 June 2004; revised 8 April 2005)

ABSTRACT

The absorption properties of the water vapor continuum and a number of weak bands for H₂O, O₂, CO₂, CO, N₂O, CH₄, and O₃ in the solar spectrum are incorporated into the Fu-Liou radiation parameterization program by using the correlated k -distribution method (CKD) for the sorting of absorption lines. The overlap absorption of the H₂O lines and the H₂O continuum (2500–14500 cm⁻¹) are treated by taking the two gases as a single-mixture gas in transmittance calculations. Furthermore, in order to optimize the computation efforts, CO₂ and CH₄ in the spectral region 2850–5250 cm⁻¹ are taken as a new single-mixture gas as well. For overlap involving other absorption lines in the Fu-Liou spectral bands, the authors adopt the multiplication rule for transmittance computations under which the absorption spectra for two gases are assumed to be uncorrelated. Compared to the line-by-line (LBL) computation, it is shown that the errors in fluxes introduced by these two approaches within the context of the CKD method are small and less than 0.48% for the H₂O line and continuum in the 2500–14500 cm⁻¹ solar spectral region, ~1% for H₂O (line)+H₂O (continuum)+CO₂+CH₄ in the spectral region 2850–5250 cm⁻¹, and ~1.5% for H₂O (line)+H₂O (continuum)+O₂ in the 7700–14500 cm⁻¹ spectral region. Analysis also demonstrates that the multiplication rule over a spectral interval as wide as 6800 cm⁻¹ can produce acceptable errors with a maximum percentage value of about 2% in reference to the LBL calculation. Addition of the preceding gases increases the absorption of solar radiation under all sky conditions. For clear sky, the increase in instantaneous solar absorption is about 9%–13% (~12 W m⁻²) among which the H₂O continuum produces the largest increase, while the contributions from O₂ and CO₂ rank second and third, respectively. In cloudy sky, the addition of absorption amounts to about 6–9 W m⁻². The new, improved program with the incorporation of the preceding gases produces a smaller solar absorption in clouds due to the reduced solar flux reaching the cloud top.

Key words: non-gray gas absorption, correlated k -distribution method, Fu-Liou code

1. Introduction

The absorption of a number of gases in the earth's atmosphere makes an important contribution to the radiation budget of the Earth-atmosphere system. In the discussion of solar absorption, Liou (2002) presented numerous solar absorption bands of gases that have not been properly accounted for in radiation parameterizations. These include absorption lines associated with H₂O, CO₂, O₃, O₂, N₂O, CH₄, CO, and NO₂. It is noted that only the major absorbers (H₂O near-infrared bands, O₂, CO₂ near-infrared bands, and

O₃ UV and visible bands) have been considered in the radiative transfer parameterizations in the majority of current general circulation models (GCMs). A common feature in most GCMs to date has shown that the simulated net solar fluxes at the top of the atmosphere (TOA) are smaller than the observed values, indicating a cold bias in the GCMs (Gu et al., 2003). Introducing the neglected absorbers in the radiation model can correct this cold bias and at the same time improve the performance of the GCMs.

Thus, the objective of the present study is to investigate the role of the aforementioned absorbing gases

*E-mail: zfsu@mail.iap.ac.cn

within the context of the Fu-Liou radiation parameterization program in both clear and cloudy atmospheres (Fu and Liou, 1992, 1993; Charlock and Alberta, 1996) for application to climate models (e.g., the UCLA (University of California, Los Angeles) and IAP (Institute of Atmospheric Physics) GCMs). To this end, we have incorporated in this program the following solar absorption bands: H₂O continuum (0.69–4.0 μm); H₂O visible band; O₂ A band (0.76 μm), B band (0.69 μm), γ band (0.63 μm), 1.06, 1.27, and 1.58 μm bands; CO₂ 1.4, 1.6, 2.0 and 2.7 μm bands; CO 2.34 μm band; N₂O 2.87 and 2.97 μm bands; CH₄ 3.83, 3.53, 3.31, 3.26, 2.37, 2.30, 2.20, and 1.66 μm bands; and O₃ 3.3 μm band.

The present paper is organized as follows. In section 2, we discuss the incorporation of the absorption properties of a number of trace gases within the context of the correlated k -distribution method, in which the data sources used, the treatment of overlap, and verification are presented. In section 3, we present a comparison of the flux and heating rate computed from the new version of the Fu-Liou radiation program to those from the original version. Conclusions are given in section 4.

2. Incorporation of new gaseous absorption based on CKD

2.1 Data description

A continuum model, which includes absorption due to water vapor, nitrogen, oxygen, carbon dioxide, and ozone, has been developed by the scientists at the Atmospheric and Environmental Research (AER) Inc., U.S.A. (Clough et al., 1989, 1992; Clough and Jacono, 1995). The water vapor continuum includes the entire self- and foreign-broadened continuum based on the model originally developed in the 1980s. Both the self- and foreign-continuum models are based on the contributions from a collision-induced component and a line-shape component. These two components were applied consistently to all water vapor lines from the microwave to the visible, and the results were summed to obtain the self- and foreign-continuum coefficients from 0 to 20000 cm^{-1} . This model should be regarded as a semi-empirical model with strong constraints provided by the known physics. The data that have been used to develop the new continuum model are primarily based on spectral atmospheric measurements. Only cases for which the characterization of the atmospheric state has been comprehensively checked have been used.

We have used this continuum model in our study to create a line-by-line (LBL) dataset to compute the absorption coefficients for the water vapor continuum. In

this continuum model, the self- and foreign-broadened continua of water vapor have been treated differently. However, by using control parameters, the model can also produce the total optical depth that includes both the self- and foreign-broadened continua. On the basis of the total optical depth, we can then obtain the absorption coefficient through the known water vapor amount. In this study, we have employed a spectral resolution of 0.025 cm^{-1} for the water vapor continuum absorption in consideration of the balance between accuracy and computational efficiency.

For the H₂O, CO₂, O₂, O₃, N₂O, CH₄, and CO lines, the 2000 HITRAN (High-resolution Transmission Molecular Absorption) dataset was used for the calculation of their absorption coefficients based on the following equation (Arking and Grossman, 1972; Chou and Kouvaris, 1986):

$$k(\nu, p, T) = \sum_i S_i(T) f_i(\nu, p, T), \quad (1)$$

where ν is the wavenumber, p is the air pressure, T is the air temperature, S_i is the line intensity for the i th line, and f_i is the normalized line shape. The line intensity S_i is given by (Fu and Liou, 1992)

$$S_i(T) \approx S_i(T_0) \left(\frac{T_0}{T} \right)^m \times \frac{Q_\nu(T_0)}{Q_\nu(T)} \frac{1 - \exp(-hc\nu_{ij}/KT)}{1 - \exp(-hc\nu_{ij}/KT_0)} \times \exp \left[-\frac{hcE_i}{K} \left(\frac{1}{T} - \frac{1}{T_0} \right) \right], \quad (2)$$

where $T_0=296$ K, $m=1.5$ and 1.0 for nonlinear and linear molecules, respectively, Q_ν is the vibrational partition function which is close to 1 (McClatchey et al., 1973), ν_{ij} is the wavenumber for the line center, E_i is the energy of the lower state, h is the Planck constant, K is the Boltzmann constant, and c is the velocity of light. The parameters $S_i(T_0)$, $Q_\nu(T_0)$, ν_{ij} , and E_i were taken from the 2000 HITRAN dataset. Following Chou and Kouvaris (1986), the lines have been cut off at ($260\alpha_L, 5\alpha_D$) from the line centers, where α_L is the Lorentz half-width, and α_D is the Doppler half-width. In the computations, we used the three temperatures of 190, 245, and 300 K, along with eleven pressures with $\Delta \log p=0.2$. Using Eqs. (1) and (2), we can then obtain the absorption coefficients $k(\nu, p, T)$ for the eleven pressures and three temperatures.

The absorption coefficients $k(\nu, p, T)$ were then employed to determine the cumulative probability function, $g(k, p, T)$, at the eleven pressures and three temperatures. Because g is a monotonically increasing and smooth function in k space for a given pressure and temperature, $k(g, p, T)$ can be readily obtained at the three temperatures and eleven pressures. Fu and Liou (1992) pointed out that in the CKD method,

the cumulative probability function g can replace the wavenumber ν as an independent variable in transmittance calculations. To facilitate the computation of $k(g, p, T)$ for any pressures and temperatures, the following parameterization developed by Fu and Liou (1992) was employed:

$$\ln k(g, p, T) = \sum_{n=0}^2 A_n(g, p)(T - 250)^n. \quad (3)$$

The coefficients $A_n(g, p)$ ($n = 0, 1, 2$) can be determined by the 3 temperature values. $k(g, p, T)$ for a given g and p has been tabulated at eleven pressures. For other pressures, a linear interpolation in the pressure coordinate can be followed.

2.2 Treatment of the overlap of absorption bands

The Fu-Liou solar radiation parameterization program was divided into six bands in which substantial absorption overlaps take place. In band six (2500–2850 cm^{-1}), the CH_4 3.83 and 3.53 μm bands overlap with the wing region of the H_2O 3.2 μm band. In band five (2850–4000 cm^{-1}), overlap occurs in the CH_4 3.31 and 3.26 μm bands, the O_3 3.3 μm band, and the H_2O 3.2 μm band, as well as in the CO_2 2.7 μm band, the H_2O 2.7 μm band, and the N_2O 2.97 and 2.87 μm bands. In band four (4000–5250 cm^{-1}), the CO_2 2.0 μm band overlaps with the H_2O 1.87 μm band, while the CH_4 2.37, 2.30, and 2.20 μm bands, the CO 2.34 μm band, and the wing region of the H_2O 2.7 μm band overlap each other. In band three (5250–7700 cm^{-1}), overlap is seen in the CO_2 1.6 μm band, the O_2 1.58 μm band, and the wing regions of the H_2O 1.38 and 1.87 μm bands. The CO_2 1.4 μm band also overlaps with the H_2O 1.38 μm band, while the CH_4 1.66 μm band overlaps with the wing region of the H_2O 1.87 μm band. In band two (7700–14500 cm^{-1}), the O_2 1.06 μm band overlaps with the H_2O 1.1 μm band, and the O_2 B band overlaps with the H_2O 0.72 μm band. In band one (14500–50000 cm^{-1}), the O_3 visible band, the H_2O visible band, and the O_2 0.63 μm band overlap each other.

Domoto (1974) and Wang and Ryan (1983) illustrated the importance of treating overlap absorption in radiative transfer calculations and climate studies. Goody et al. (1989), Lacis and Oinas (1991), Fu and Liou (1992), and Shi (1998) pointed out that overlap absorption by several different gases is an important theoretical and practical problem in CKD, especially when it is applied to the scattering atmosphere. Lacis and Oinas (1991) adopted the multiplication rule for transmittance computations under which the absorption spectra for two gases are assumed to be uncor-

related. Shi (1998) pointed out that overlap of numerous absorption bands can be accurately treated by using CKD. Mlawer et al. (1997) developed a method to treat bands containing gases with overlap absorption, in which the key absorbers in each spectral band are treated with high accuracy, whereas a less detailed procedure is employed to compute absorption due to minor gases in the band. In Fu and Liou (1992), two different approaches were employed to treat overlap absorption in the g space. These approaches have been proven to be both efficient and accurate for treating the overlap problem involving atmospheric radiative transfer. Since this study is based on the Fu-Liou radiation program for flux and heating rate calculations, we apply these approaches to trace gases that have not been included in the calculation of solar radiative transfer. We shall outline these two approaches below in association with the present study.

The mean transmittance involving the two different gases for a given spectral interval $T_{\bar{\nu}}(1, 2)$ can be expressed as follows:

$$T_{\bar{\nu}}(1, 2) = \int_{\Delta\nu} T_{\nu}(1) \times T_{\nu}(2) \frac{d\nu}{\Delta\nu}, \quad (4)$$

where T_{ν} the transmittance for one gas for a given wavenumber, the numbers 1 and 2 denote two different gases. The first approach is based on the assumption that $T_{\nu}(1)$ and $T_{\nu}(2)$ are uncorrelated such that $T_{\bar{\nu}}(1, 2)$ can be written as

$$T_{\bar{\nu}}(1, 2) = \int_{\Delta\nu} T_{\nu}(1) \frac{d\nu}{\Delta\nu} \times \int_{\Delta\nu} T_{\nu}(2) \frac{d\nu}{\Delta\nu} = T_{\bar{\nu}}(1) \times T_{\bar{\nu}}(2). \quad (5)$$

Using Eq. (5), the mean transmittance in the g space can be expressed in the form

$$\begin{aligned} T_{\bar{\nu}}(1, 2) &= \int_0^1 \exp\left(-\int_{z_1}^{z_2} k_1 \rho_1 dz\right) dg_1 \\ &\times \int_0^1 \exp\left(-\int_{z_1}^{z_2} k_2 \rho_2 dz\right) dg_2 \\ &\approx \sum_{m=1}^M \sum_{n=1}^N \exp(-\tau_{mn}) \Delta g_{1m} \Delta g_{2n}, \quad (6) \end{aligned}$$

where

$$\tau_{mn} = \int_{z_1}^{z_2} (k_{1m} \rho_1 + k_{2n} \rho_2) dz, \quad (7)$$

and ρ_1 and ρ_2 are the densities for gases 1 and 2, respectively; k_{1m} and k_{2n} are the respective absorption coefficients; and m and n denote the number of g values for the two gases. It is clear that Eqs. (6) and (7) allow us to use the equivalent k functions of individual gases to resolve the overlap problem.

The statistical independence for the absorption lines is an assumption and generally applicable to a narrow spectral interval. However, it is the essence of the radiative transfer parameterization to optimize the computational effort by applying this concept to spectral bands as wide as possible to make the broadband radiation program effective and efficient for use in climate and weather models. Fu and Liou (1992) concluded that the multiplication approach for overlap gases can achieve excellent accuracy in flux and heating rate calculations over a spectral interval of about 150 cm^{-1} .

In the second approach, a new absorption coefficient, which can be considered as the absorption coefficient for a single-mixture gas, is defined. Using the multiplication property, which is exact for a given wavenumber, the total optical depth $\tau(\nu)$ may be written in the form

$$\tau(\nu) = \sum_i \tau_i(\nu) = \int k(\nu, p, T) \rho dz, \quad (8)$$

where we define

$$k(\nu, p, T) = \sum_i q_i k_i(\nu, p, T), \quad (9)$$

where ρ is the air density, q_i is the mixing ratio of gas i , and $k_i(\nu, p, T)$ is the absorption coefficient of gas i at pressure p , temperature T , and wavenumber ν . The summation symbol implies the sum for all overlap gases in one band. The term $k(\nu, p, T)$ is referred to as the absorption coefficient for a single-mixture gas. Fu and Liou (1992) pointed out that the CKD method for a single-mixture gas requires the same correlated assumptions as those for an individual gas. However, if we consider the overlap absorption of H_2O with other gases, one additional variable, namely the H_2O mixing ratio q , is needed. Moreover, to facilitate the computation of $k(g, p, T, q)$, the following parameterization has been developed:

$$k(g, p, T, q) = \exp \left[\sum_{n=0}^2 A_n(g, p) (T - 250)^n \right] + q \exp \left[\sum_{n=0}^2 B_n(g, p) (T - 250)^n \right], \quad (10)$$

where the coefficients A_n and B_n ($n = 0, 1, 2$) are determined by three temperatures, two H_2O mixing ratios, and eleven pressures in the g -domain. The second approach does not require the assumption that the two absorption spectra are uncorrelated, and it is computationally more efficient.

The H_2O lines and H_2O continuum have been treated as two different gases in this study, but we do not know whether these two absorption spectra are

uncorrelated. Thus, the second approach has been followed in which the CKD method for this new single-mixture gas requires the same correlated assumption as that for an individual gas, except that one additional variable, namely the H_2O mixing ratio q , has been added. The absorption coefficient for this new single-mixture gas is:

$$k(\nu, p, T, q) = qk_1(\nu, p, T) + qk_2(\nu, p, T), \quad (11)$$

where $k_1(\nu, p, T)$ and $k_2(\nu, p, T)$ are the absorption coefficients of H_2O (line) and H_2O (continuum), respectively, and q is the H_2O mixing ratio. On the basis of Eq. (10), we have developed the following parameterization:

$$k(g, p, T, q) = q \exp \left[\sum_{n=0}^2 B_n(g, p) (T - 2500)^n \right], \quad (12)$$

where B_n ($n = 0, 1, 2$) are determined by three temperatures and one H_2O mixing ratio for 11 pressures in the g -space.

Furthermore, in order to economize the computation effort, in the $2850\text{--}5250 \text{ cm}^{-1}$ spectral region, CO_2 and CH_4 have been taken as a new single-mixture gas. The absorption coefficient for this new gas is given by

$$k(\nu, p, T) = q_1 k_1(\nu, p, T) + q_2 k_2(\nu, p, T), \quad (13)$$

where $k_1(\nu, p, T)$ and $k_2(\nu, p, T)$ are the absorption coefficients of CH_4 and CO_2 , respectively; and q_1 and q_2 are the mixing ratios for these two gases, which have been taken as constants in this study. The CKD method for this new single-mixture gas requires the same correlated assumption as that for an individual gas.

In this study, we have used an LBL model to verify the accuracy of the parameterization. The "exact" LBL calculation for fluxes covering the entire solar spectrum ($\sim 0.2\text{--}5 \mu\text{m}$) would be a formidable computational task. Moreover, many LBL models even with the same input line parameters and atmospheric profiles have shown to provide diverse accuracy in comparison to ground-based spectral radiance observations. In conjunction with the present broadband study and after trial-and-error, we have used a 0.025 cm^{-1} spectral interval to perform the LBL calculations. The selection of this interval is also in line with that suggested by Chou and Kouvaris (1986) for flux calculations.

Tables 2 and 3 show the LBL results for the overlap absorption of H_2O lines with CO_2 and CH_4 lines in the $2850\text{--}5250 \text{ cm}^{-1}$ spectral region, and with O_2 lines in the $7700\text{--}14500 \text{ cm}^{-1}$ region, respectively. From Table 2, we see that the maximum effects of the CO_2 and CH_4 lines on flux calculations are 2.20 and 1.22 W m^{-2} , respectively. If the second approach is used,

Table 1. The optimum number of g values in the correlated k -distribution method.

Spectral region (0.2–4.0 μm)	Number of quadrature points							
	H ₂ O	O ₂	O ₃	CO ₂	CO	N ₂ O	CH ₄	H ₂ O (continuum)
0.2–0.69	10	1	10					
0.69–1.3	12	12						12
1.3–1.9	12	1		12			1	12
1.9–2.5	20			20	1		20	20
2.5–3.5	20		1	20		1	20	20
3.5–4.0	20						1	20

Table 2. The LBL calculation of the absorption of solar radiation by H₂O, CO₂, and CH₄ in the solar band 2850–5250 cm^{-1} . The solar zenith angle used is 60° and the surface albedo is set to zero. The units are in W m^{-2} .

Atmospheric profiles	CO ₂	H ₂ O	H ₂ O+CO ₂	H ₂ O+CO ₂ +CH ₄	CO ₂	CH ₄
MLS	6.36	22.41	24.04	24.94	1.63	0.90
SAW	6.14	15.72	17.92	19.14	2.20	1.22
TRO	6.39	23.52	25.03	25.86	1.51	0.83
USS	6.29	20.00	21.85	22.89	1.85	1.04

Table 3. The LBL calculation of the absorption of solar radiation by H₂O and O₂ in the solar band 7700–14500 cm^{-1} . The solar zenith angle used is 60° and the surface albedo is set to zero. The units are in W m^{-2} .

Atmospheric profiles	O ₂	H ₂ O	H ₂ O+O ₂	O ₂
MLS	3.41	45.95	49.35	3.40
SAW	3.40	17.12	20.52	3.40
TRO	3.41	52.81	56.20	3.39
USS	3.41	33.02	36.42	3.40

we find that the absorption contribution of these CO₂ and CH₄ bands has been significantly suppressed by that of H₂O. For this reason, the first approach has been used to calculate the mean transmittance in the g space for the overlap absorption between H₂O and CO₂+CH₄. Based on the comparison to the LBL result, we will show that the first approach has produced acceptable error for overlap absorption of CO₂ and CH₄ with other gases in the spectral region 2850–5250 cm^{-1} . Moreover, in the spectral regions 5250–7700 cm^{-1} and 2500–2850 cm^{-1} , the first approach with only one quadrature point has been used to deal with the overlap absorption of CH₄ due to its small effects.

The overlap absorption by H₂O and O₂ in the 7700–14500 cm^{-1} spectral region is small because the O₂ 0.76 and 0.69 μm bands are located in the windows between the H₂O bands (Table 3). The absorption spectra for H₂O and O₂ appear to be uncorrelated, so it is reasonable to use the first approach to treat their overlap absorption. The LBL calculation shows that the effect of the O₂ 1.58 μm band is very small, that the solar absorption by the O₂ γ band contributes about 0.56 W m^{-2} , and that the maximum overlap ef-

fects of the CO 2.34 μm band, N₂O 2.87 and 2.97 μm bands, and O₃ 3.3 μm band are about 0.01, 0.05, and 0.02 W m^{-2} , respectively (not shown in the tables). It is clear that the overlap effects of the O₂ 1.58 μm and γ bands, CO, O₃, and N₂O bands are largely overshadowed by the H₂O (including continuum) absorption. To optimize the computation efforts, we have followed the first approach using only one quadrature point (seen Table 1) for the overlap problem of the O₂ 1.58 μm and γ bands, and the CO, O₃, and N₂O bands.

In summary, for overlap of the H₂O lines and H₂O continuum in the 2500–14500 cm^{-1} spectral region, we follow the approach of a single-mixture gas (the second approach) for the transmittance calculations, which requires the same correlated assumptions as those for an individual gas except that one more variable, namely the H₂O mixing ratio q , is needed, to optimize the computation effort. However, we adopt the multiplication rule (the first approach) for the computation of spectral transmittances under which the gaseous absorption spectra are assumed to be uncorrelated to deal with the following overlap absorption:

H₂O (including continuum) and CH₄ in band six; H₂O (including continuum), O₃, N₂O, and (CO₂+CH₄) in band five; H₂O (including continuum), CO, and (CO₂+CH₄) in band four; H₂O (including continuum), CO₂, CH₄, and O₂ in band three; H₂O (including continuum) and O₂ in band two; and the H₂O visible band, the O₃ visible band, and the O₂ 0.63 μ m band in band one. It should be noted that in order to optimize the computation efforts, in band four and band five (2850–5250 cm⁻¹), CO₂ and CH₄ have been taken as a new single-mixture gas requiring the same correlated assumption as that for an individual gas. Moreover, to economize the computation effort and at the same time to achieve acceptable accuracy, we have employed one quadrature point for the O₃ 3.3 μ m band, CO 2.34 μ m band, and N₂O bands, the CH₄ 3.83, 3.53, and 1.66 μ m bands, and the O₂ 1.58 μ m and γ bands. The optimum numbers of g values are displayed in Table 1.

It should be pointed out that, for the overlap problem between strong and weak absorptions, the second approach, which introduces a new single-mixture gas, is unsuitable since the contribution of weak absorption will be greatly suppressed by that of the strong one. Moreover, it would be unreasonable to assume that the water vapor line and continuum are uncorrelated. Thus, the first method (i.e. multiplication rule) is not applicable to the overlap problem involving water vapor line and continuum absorption.

2.3 Verification of the accuracy of the parameterization of the new trace gases

Our main objective is to investigate the optimum

number of g values that would produce the flux results within $\sim \pm 1\%$ below ~ 30 km for all these new gases mentioned before. In flux and heating rate calculations, the same formulas in Fu and Liou (1992) [Eqs. (4.4)–(4.8)] have been used. And in the calculations, the mixing ratios for CO₂, CH₄, N₂O, O₂, and CO were assumed to be uniform throughout the atmosphere with concentrations of 330, 1.6, 0.28, 2.0948×10^5 , 0.16 ppmv, respectively. The water vapor and O₃ mixing ratios were assumed to be linear in the height coordinate in terms of the logarithmic scale. Four atmospheric profiles, including the midlatitude summer (MLS), subarctic winter (SAW), tropical (TRO) and U.S. Standard atmospheres (USS) (McClatchey et al., 1971) have been used in flux and heating rate calculations.

There are two sets of errors used in determining the accuracy of CKD. First, for the downward flux at the surface, the outgoing flux at the top of the atmosphere, and the flux absorbed by gases, the difference between the exact (F_{LBL}) and approximate result (F) is expressed as a percentage error, defined by $E_F = 100(F - F_{\text{LBL}})/F_{\text{LBL}}$. Second, for the heating/cooling rates throughout the atmosphere, the difference between the exact (H_{LBL}) and approximate result (H) is expressed as the absolute error, defined by $E_H(z) = H(z) - H_{\text{LBL}}(z)$.

Tables 4, 5, and 6 illustrate comparisons of the downward flux at the surface $F^\downarrow(0)$ and the absorbed fluxes F_a between the CKD and LBL methods for the overlap absorption of the H₂O lines and H₂O conti-

Table 4. Comparison of the LBL and CKD methods for the surface and absorbed fluxes due to overlap absorption bands of H₂O lines and H₂O continuum in the solar spectral region 2500–14500 cm⁻¹. The surface albedo is set to zero. The percentage error is shown in parentheses. The units are in W m⁻².

	Atmospheric profile	$F^\downarrow(0)$		F_a	
		LBL	CKD	LBL	CKD
$\theta_0 = 30^\circ$	MLS	455.19	455.40 (0.05)	168.61	168.40 (-0.13)
	SAW	531.89	532.21 (0.06)	91.91	91.59 (-0.36)
	TRO	438.83	439.09 (0.06)	184.97	184.71 (-0.14)
	USS	487.30	487.70 (0.08)	136.50	136.10 (-0.29)
$\theta_0 = 60^\circ$	MLS	247.80	248.08 (0.11)	112.36	112.07 (-0.25)
	SAW	296.88	297.07 (0.06)	63.27	63.09 (-0.29)
	TRO	237.71	238.19 (0.20)	122.44	121.97 (-0.39)
	USS	268.04	268.23 (0.07)	92.11	91.93 (-0.20)
$\theta_0 = 75^\circ$	MLS	118.31	118.63 (0.28)	68.12	67.80 (-0.48)
	SAW	146.45	146.56 (0.08)	39.98	39.87 (-0.28)
	TRO	112.78	113.04 (0.23)	73.65	73.39 (-0.35)
	USS	129.62	129.77 (0.07)	56.81	56.66 (-0.26)

Table 5. Comparison of the LBL and CKD methods for the surface and absorbed fluxes due to overlap absorption bands of H₂O (line)+H₂O (continuum)+O₂ in the solar spectral region 7700–14500 cm⁻¹. The solar zenith angle used is 60°, while the surface albedo is set to zero. The percentage error is shown in parentheses. The units are in W m⁻².

Atmospheric profile	$F^\downarrow(0)$		F_a	
	LBL	CKD	LBL	CKD
MLS	190.12	190.91 (0.42)	52.02	51.22 (-1.54)
SAW	220.59	221.00 (0.19)	21.55	21.14 (-1.90)
TRO	183.04	183.96 (0.50)	59.10	58.18 (-1.56)
USS	203.67	204.25 (0.28)	38.47	37.89 (-1.51)

Table 6. Comparison of the LBL and CKD methods for the surface and absorbed fluxes due to overlap absorption bands of H₂O (line)+H₂O (continuum)+CO₂+CH₄ in the solar spectral region 2850–5250 cm⁻¹. The solar zenith angle used is 60°, while the surface albedo is set to zero. The percentage error is in parentheses. The units are in W m⁻².

Atmospheric profile	$F^\downarrow(0)$		F_a	
	LBL	CKD	LBL	CKD
MLS	14.37	14.18 (-1.32)	25.82	26.01 (0.74)
SAW	20.17	19.90 (-1.34)	20.02	20.29 (1.35)
TRO	13.46	13.32 (-1.04)	26.74	26.87 (0.49)
USS	16.42	16.25 (-1.04)	23.77	23.94 (0.72)

num, H₂O (including continuum) and O₂, and H₂O (including continuum), CO₂, and CH₄, respectively. From Table 4, it is clear that by using the second approach, the CKD has achieved very high accuracy for the overlap absorption of the H₂O lines and H₂O continuum. For the absorbed solar flux, errors are less than -0.36% (-0.32 W m⁻²) for the solar zenith angle of 30°, while for the solar zenith angles of 60° and 75°, the maximum errors for absorption are -0.39% (-0.47 W m⁻²) and -0.48% (-0.32 W m⁻²), respectively.

Using the first approach, Ackerman (1979) demonstrated that the error introduced by multiplying the two transmittances is not likely to be of significance for a 5 cm⁻¹ spectral width. Furthermore, Fu and Liou (1992) pointed out that using Eq. (2.3) for overlap gases over a spectral interval of ~150 cm⁻¹ can achieve excellent accuracy in flux and heating rate calculations (within ~1.0%). In this study, we have used the first approach for spectral intervals as large as 2400 cm⁻¹ for CO₂ and 6800 cm⁻¹ for O₂ for speedy computations. From Table 5, it is seen that the maximum absolute percentage errors for the fluxes are less than 1.9%. However, these errors are greatly suppressed by strong overlap absorption with the H₂O lines and H₂O continuum over these spectral bands. From Table 6, it is clear that the first approach has produced excellent results with a percentage error ~1% for the overlap absorption bands of H₂O (including continuum) and CO₂ and CH₄ in the 2850–5250 cm⁻¹ spectral region.

Figures 1, 2a–b, and 2c–d show the heating rate profiles computed from LBL and the error profiles produced by CKD for the overlap absorption bands of the H₂O continuum and H₂O lines in the 2500–14500 cm⁻¹ spectral region, H₂O (including continuum) and CO₂ and CH₄ in 2850–5250 cm⁻¹, and H₂O (including continuum) and O₂ in 7700–14500 cm⁻¹. For the spectral region 2500–14500 cm⁻¹, the heating rate errors below 40 km are less than 0.05 K d⁻¹ in reference to the LBL results, while those above 40 km are less than 0.09 K d⁻¹. For the 2850–5250 cm⁻¹ spectral region, the heating rate results agree with those from LBL within ~0.05 K d⁻¹ up to 50 km. The heating rate errors for the spectral region 7700–14500 cm⁻¹ are less than 0.05 K d⁻¹ below about 40 km but slightly larger above this height. The maximum difference of ~0.3 K d⁻¹ that occurs at about 50 km is probably due to the multiplication approximation. The aforementioned comparison demonstrates that CKD is a reliable approach for flux and heating rate calculations for these bands. The present radiation parameterization program has been applied to the IAP AGCM 9L whose top level is set to about 30 km, and would also be suitable for application to GCMs with a top model level of about 50 km. Results not shown here also reveal excellent accuracies for the H₂O visible, CO, CH₄, N₂O, O₂, and O₃ bands.

In summary, using the parameterization developed above, we have incorporated the preceding absorption bands not previously accounted for into the Fu-Liou

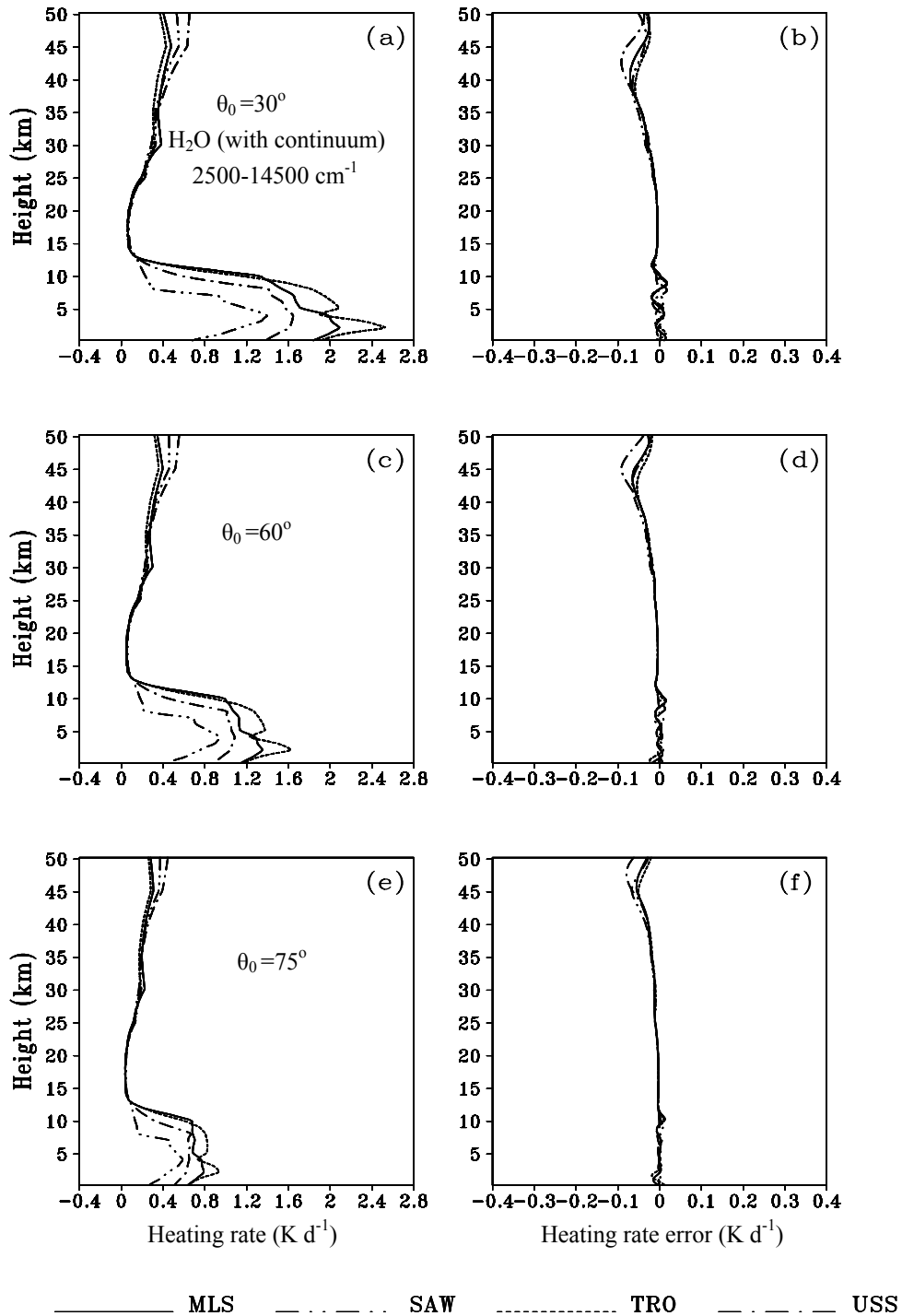


Fig. 1. The heating rate profiles computed from LBL (left panels) and the error profiles produced by CKD (right panels) for overlap absorption bands of H₂O continuum and H₂O lines in the solar spectrum 2500–14500 cm⁻¹ in the midlatitude summer (MLS, solid), subarctic winter (SAW, double-dot dashed), tropical (TRO, dashed), and U.S. Standard (USS, dot-dashed) atmospheres. θ_0 is the solar zenith angle. (a, b) $\theta_0 = 30^\circ$; (c, d) $\theta_0 = 60^\circ$; (e, f) $\theta_0 = 75^\circ$. The surface albedo is set to zero. The units are in K d⁻¹.

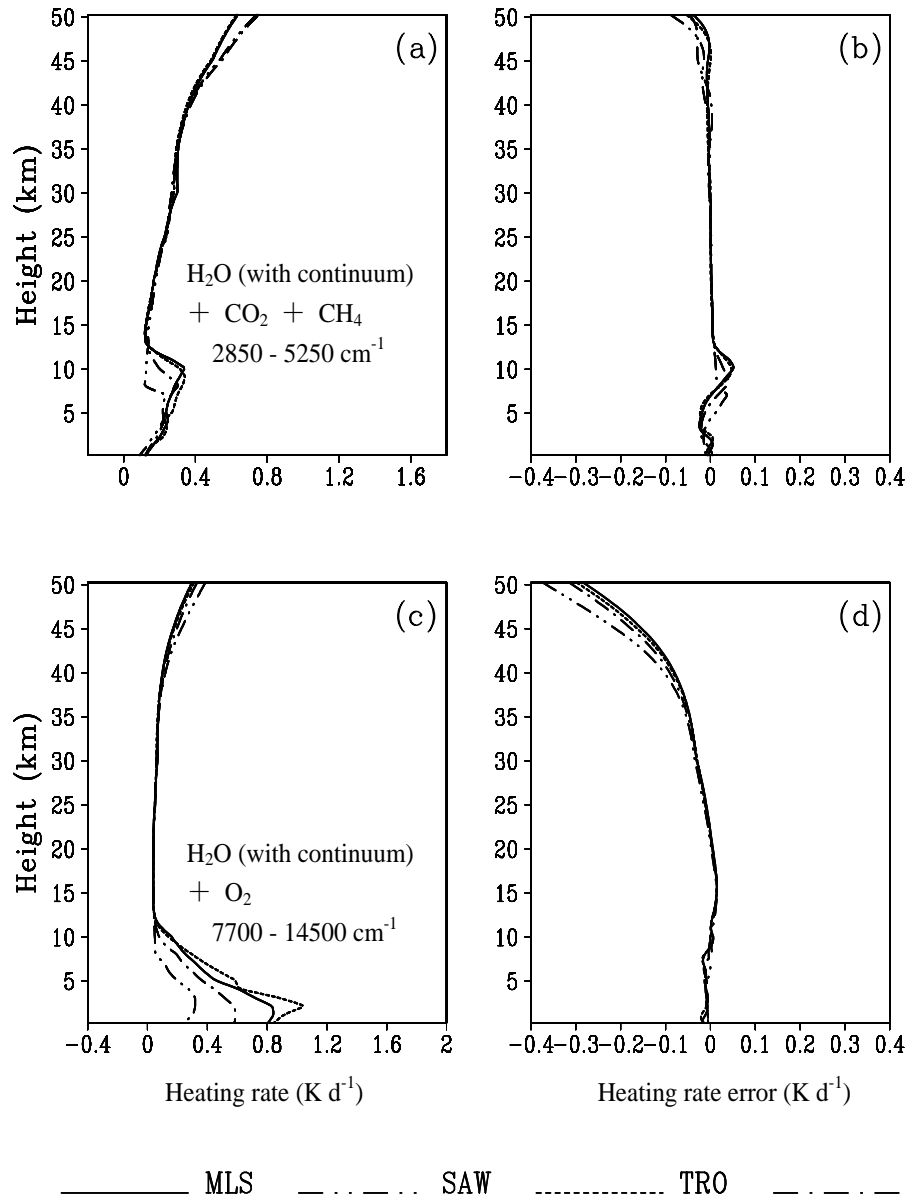


Fig. 2. The heating rate profiles computed from LBL and the error profiles produced by CKD for (a, b) overlap absorption of H₂O continuum, H₂O lines, and CO₂ in the solar spectrum 2850–5250 cm⁻¹, and (c, d) H₂O continuum, H₂O lines, and O₂ in the solar spectrum 7700–14500 cm⁻¹ in the midlatitude summer (MLS, solid), subarctic winter (SAW, dashed double-dotted), tropical (TRO, dashed), and U.S. Standard (USS, dot-dashed) atmospheres. The solar zenith angle used is 60° and the surface albedo is set to zero. The units are in K d⁻¹.

radiation program, which is referred to as the new version. In the next section, we present some illustrative results regarding the effect of these gases on flux and heating rate calculations.

3. Results and discussions

In clear sky, results of the contribution of solar absorption produced by the new absorption bands have

shown that for different solar zenith angles the relative increases are more than 9% for all four atmospheric profiles. The individual effects on the clear sky flux in the new version are given in Table 7. We see that the H₂O continuum generates the largest solar absorption, followed by the absorption of O₂, CO₂, H₂O visible band, and CH₄. The contributions of N₂O, O₃ 3.3 μm band and CO on solar absorption are quite small and can be neglected for most practical applications. It

Table 7. The individual contribution of the new absorption bands to the solar absorption flux in clear sky calculated by the Fu-Liou code. The solar zenith angle is set to 60° and the surface albedo is set to 0.1. The units are in W m^{-2} .

	MLS	SAW	TRO	USS
H ₂ O (continuum)	5.04	3.81	5.29	4.48
CO ₂	2.30	2.39	2.14	2.67
O ₂	2.72	3.15	2.62	2.91
H ₂ O visible band	1.87	0.30	2.55	0.97
CH ₄	0.57	0.84	0.53	0.66

Table 8. Comparison of $F^\downarrow(0)$, $F^\uparrow(\text{TOA})$ and F_a between the new and old versions of the Fu-Liou code. The solar zenith angle used is 60° and the surface albedo is 0.1. The difference (new version – old version) is shown in parentheses. The units are in W m^{-2} .

Atmospheric profiles		$F^\downarrow(0)$		$F^\uparrow(\text{TOA})$		F_a	
		Old	New	Old	New	Old	New
Clear sky	MLS	491.7	479.6 (–12.1)	89.27	87.64 (–1.63)	132.21	144.71 (12.50)
	SAW	535.0	523.8 (–11.2)	92.97	91.56 (–1.41)	89.53	101.02 (11.49)
Low cloud	MLS	50.42	49.54 (–0.88)	461.3	452.1 (–9.2)	157.33	167.30 (9.97)
	SAW	52.10	51.60 (–0.50)	481.7	473.5 (–8.2)	135.41	144.02 (8.61)
Middle cloud	MLS	43.22	42.60 (–0.62)	498.3	492.1 (–6.2)	126.78	133.55 (6.77)
	SAW	44.20	43.81 (–0.39)	496.7	489.9 (–6.8)	127.53	134.72 (7.19)
High cloud	MLS	417.9	408.1 (–9.8)	160.5	158.9 (–1.6)	127.31	137.80 (10.49)
	SAW	452.6	443.9 (–8.7)	161.5	159.8 (–1.7)	95.17	104.66 (9.49)
Three cloud layers	MLS	21.37	20.85 (–0.52)	510.7	505.1 (–5.6)	134.05	140.13 (6.08)
	SAW	21.92	21.69 (–0.23)	507.8	501.7 (–6.1)	136.52	142.83 (6.31)

has been noted that the solar absorption due to the H₂O visible band largely depends on temperature. In colder (warmer) conditions, the H₂O visible band absorbs less (more) solar radiation.

In the following, we present the heating rate profile, the upward flux $F^\uparrow(\text{TOA})$, and the downward flux $F^\downarrow(0)$ for five different conditions: clear sky; a single-layer low cloud (LWC=0.22 g m⁻³, $r_e=5.89 \mu\text{m}$); a single-layer middle cloud (LWC=0.28 g m⁻³, $r_e=6.2 \mu\text{m}$); a single-layer high cloud (IWC=0.0048 g m⁻³, $D_e=41.5 \mu\text{m}$); and a three-layer cloud, where LWC/IWC denotes liquid/ice water content, and r_e/D_e represents mean effective radius/width. The low cloud is positioned from 1 to 2 km in MLS and from 0.5 to 1.5 km in SAW, while the middle cloud extends from 4 to 5 km in MLS and from 2 to 3 km in SAW. The high cloud is located between 10 and 12 km in MLS and between 6 and 8 km in SAW.

Comparisons of $F^\downarrow(0)$, $F^\uparrow(\text{TOA})$, and F_a (solar absorption) between the new version and the original Fu-Liou code for the solar zenith angle of 60° are given in Table 8. Under clear and cloudy conditions, the new version produces a smaller downward flux at the surface, a smaller upward flux at the top of the atmosphere and a larger solar absorption than the original Fu-Liou code. Inclusion of the preceding new absorp-

tion bands increases solar absorption by 12.50–11.49 W m⁻² in clear sky, and by 9.97–8.61 W m⁻², 6.77–7.19 W m⁻², 10.49–9.49 W m⁻², and 6.08–6.31 W m⁻² in the low-, middle-, high-, and three-cloud conditions, respectively. The first and second numbers are for MLS and SAW, respectively. The total absorption contribution of the new bands in cloudy skies is smaller than that in clear sky. Furthermore, more solar radiation is reflected by a low or a middle cloud than by a high cloud because of the respective optical depths. In the midlatitude summer atmosphere containing a high cloud, due to more solar radiation reaching the ground, $F^\downarrow(0)$ decreases by about 9.8 W m⁻², which is larger than the decrease in $F^\uparrow(\text{TOA})$ ($\sim 1.6 \text{ W m}^{-2}$). For a low cloud or a middle cloud, due to more solar radiation being reflected, the decrease in $F^\downarrow(0)$ is only about 0.88 or 0.62 W m⁻², while for $F^\uparrow(\text{TOA})$ it is about 9.2 or 6.2 W m⁻², respectively.

Figure 3 shows the heating rate calculated from the new version of the Fu-Liou code and the difference between this and the old version under the five sky conditions mentioned above. We see that compared to the original version, the new version has a larger heating rate in clear sky throughout the whole column, whereas in cloudy sky, the new version has generated

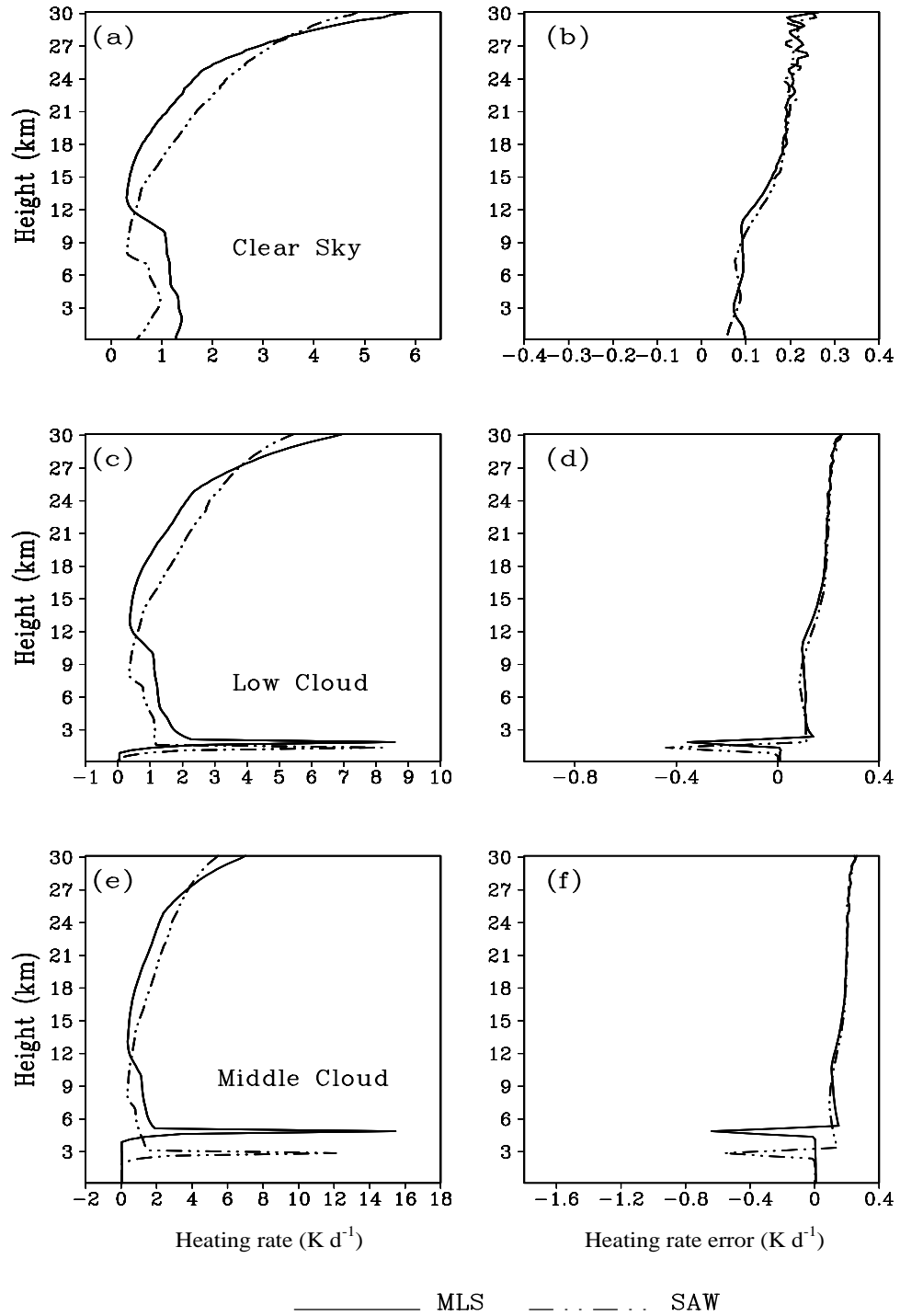


Fig. 3. The heating rate calculated from the new version of the Fu-Liou code (left panels) and the difference of heating rates between the new and old versions (new-old) (right panels). (a, b) clear sky; (c, d) low cloud; (e, f) middle cloud; (g, h) high cloud; and (i, j) three layer clouds. The solar zenith angle used is 60° and the surface albedo is set at 0.1. The solid line is for MLS, while the dashed is for SAW. The units are in $K d^{-1}$.

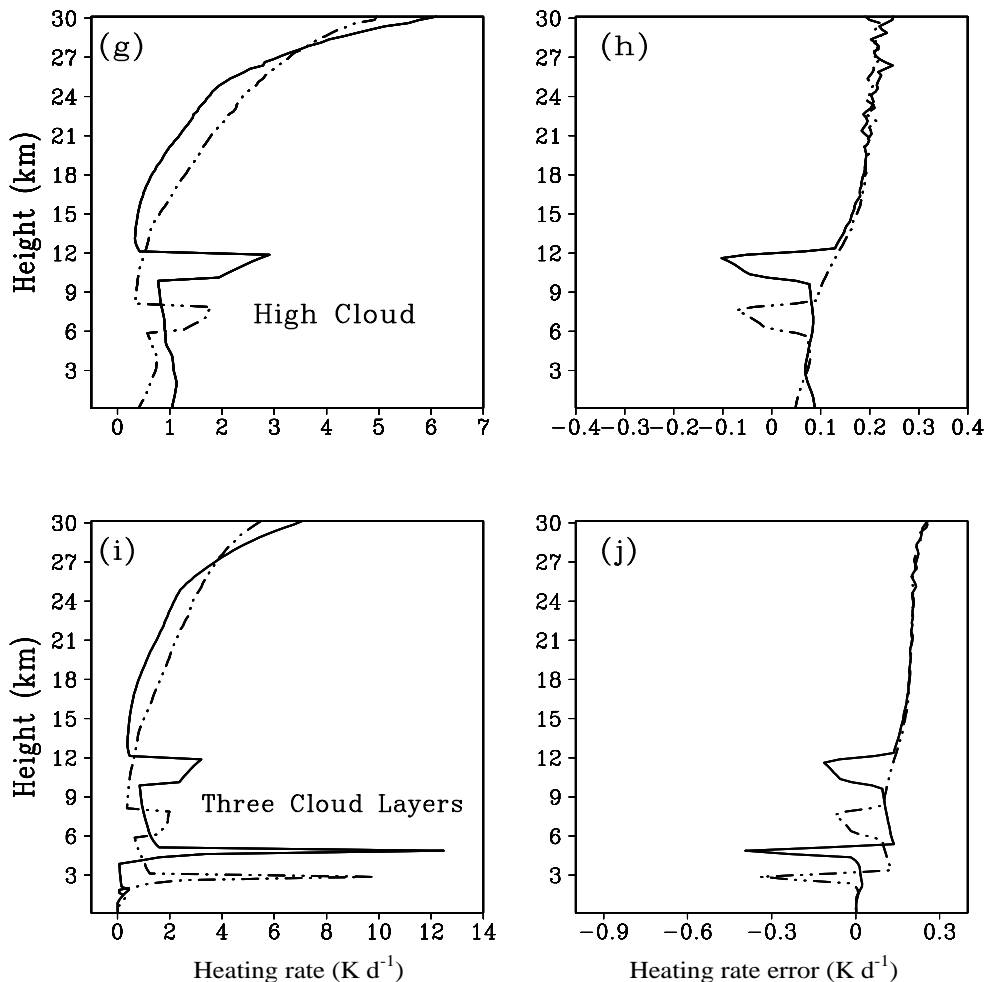


Fig. 3. (Continued).

a smaller solar absorption in clouds and a larger value above and below the clouds. The increase in solar absorption above the cloud in the new version due to inclusion of the new absorption bands is clearly dependent on the position of the cloud and its reflecting power. This increase reduces solar flux reaching the cloud top, resulting in relatively smaller cloud absorption.

Cess et al. (1996) pointed out that compared to observations, the Fu-Liou radiation program overestimates transmittances by an average of 5% in clear-sky while 11% under cloudy conditions. After introducing additional gaseous absorption into the Fu-Liou code, it is shown that $F^\downarrow(0)$ decreases in all atmospheric conditions (Table 8), revealing a decrease in the atmospheric transmittance in the modified Fu-Liou Code. Therefore, introducing more gaseous absorption has improved the performance of the Fu-Liou program and hence will enhance the accuracy of radiation field calculations in GCMs. Since only one quadrature point

has been used for most of the minor absorbing gases in weak bands to optimize the computational efforts in the parameterization, the computing time has not been significantly increased (less than 10% compared to the old version) and the radiation parameterization scheme developed in this paper is very suitable for direct application to GCMs and climate models.

4. Conclusions

In this paper, we have incorporated the absorption properties of a number of trace gases, including the water vapor continuum (0.69–4.0 μm); the H_2O visible band; the O_2 A (0.76 μm), B (0.69 μm), γ (0.63 μm), 1.06, 1.27, and 1.58 μm bands; the CO_2 1.4, 1.6, 2.0, and 2.7 μm bands; the CO 2.34 μm band; the N_2O 2.87 and 2.97 μm bands; the CH_4 3.83, 3.53, 3.31, 3.26, 2.37, 2.30, 2.20 and 1.66 μm bands; and the O_3 3.3 μm band in the Fu-Liou radiation parameterization program for the computation of fluxes and heating rates

in clear and cloudy atmospheres.

For overlap absorption of H₂O lines and H₂O continuum, we follow the approach of a single mixed gas for transmittance calculations. In order to optimize the computation efforts, in band four and band five (2850–5250 cm⁻¹), CO₂ and CH₄ have been taken as a new single-mixture gas also. The multiplication rule for the computation of spectral transmittance under which the absorption spectra for two gases are assumed to be uncorrelated is employed to treat a number of overlaps within the framework of the Fu-Liou solar radiation parameterization program. We show that the errors introduced by these two approaches within the context of the CKD method, as compared to the LBL method, are small and acceptable. Analysis also shows that the multiplication rule over spectral intervals as large as 6800 cm⁻¹ produces a small maximum error of about 1.90%.

Under all sky conditions, the new version of the Fu-Liou radiation parameterization has produced larger solar absorption than the original one. Contribution from the absorption of the H₂O continuum is most important, followed by O₂, CO₂, the H₂O visible band, and CH₄. The contributions of N₂O, the O₃ 3.3 μm band and CO on solar absorption are quite small and can be neglected for most practical applications. In cloudy sky, the new version has generated a smaller solar absorption in the cloud due to less solar flux reaching the cloud top. Finally, it is our intent to integrate the new version of the Fu-Liou radiation program into the IAP AGCM II to determine the contributions of the preceding absorption bands to the heating of the Earth-atmosphere system for climate study.

Acknowledgments. The research was financially supported by the National Natural Science Foundation of China (Grant No.40233027) and supported by the Key Knowledge Innovation Project of Chinese Academy of Sciences (Grant No: KZCX3-SW-226). During the course of this study, Zhang Feng was a scientific visitor in the Department of Atmospheric Sciences at UCLA supported in part by NSF (National Science Foundation) grants ATM-9907924 and ATM-0331550. The authors would like to thank Dr. Y. Takano for his valuable advice and suggestions.

REFERENCES

- Ackerman, T. P., 1979: On the effect of CO₂ on atmospheric heating rates. *Tellus*, **31**, 115–123.
- Arking, A., and K. Grossman, 1972: The influence of line shape and band structure on temperatures in planetary atmospheres. *J. Atmos. Sci.*, **29**, 937–949.
- Cess, R. D., M. H. Zhang, Y. Zhou, X. Jing, and V. Dvortsov, 1996: Absorption of solar radiation by clouds: Interpretations of satellite, surface, and aircraft measurements. *J. Geophys. Res.*, **101**, 23,299–23,309.
- Charlock, T. P., and T. L. Alberta, 1996: The CERES/ARM/GEWEX Experiment (CAGEX) for the retrieval of radiative fluxes with satellite data. *Bull. Amer. Meteor. Soc.*, **77**, 2673–2684.
- Chou, M. D., and L. Kouvaris, 1986: Monochromatic calculations of atmospheric radiative transfer due to molecular line absorption. *J. Geophys. Res.*, **91**, 4047–4055.
- Clough, S. A., and M. J. Iacono, 1995: Line-by-line calculation of atmospheric fluxes and cooling rates 2. Application to carbon dioxide, ozone, methane, nitrous oxide, and the halocarbons. *J. Geophys. Res.*, **100**, 16519–16535.
- Clough, S. A., F. X. Kneizys, and R. W. Davies, 1989: Line shape and the water vapor continuum. *Atmos. Res.*, **23**, 229–241.
- Clough, S. A., M. J. Iacono, and J. L. Moncet, 1992: Line-by-line calculations of atmospheric fluxes and cooling rates: Application to water vapor. *J. Geophys. Res.*, **97**, 15761–15785.
- Domoto, G. A., 1974: Frequency integration for radiative transfer problems involving homogeneous non-gray cases: The inverse transmission function. *Journal of Quantitative Spectroscopy and Radiative Transfer*, **14**, 935–942.
- Fu, Q., and K. N. Liou, 1992: On the correlated k-distribution method for radiative transfer in nonhomogeneous atmospheres. *J. Atmos. Sci.*, **49**, 2139–2156.
- Fu, Q., and K. N. Liou, 1993: Parameterization of the radiative properties of cirrus clouds. *J. Atmos. Sci.*, **50**, 2008–2025.
- Goody, R. M., R. West, L. Chen, and D. Crisp, 1989: The correlated-k method for radiation calculation in nonhomogeneous atmospheres. *Journal of Quantitative Spectroscopy and Radiative Transfer*, **42**, 539–550.
- Gu, Y., J. Farrara, K. N. Liou, and C. R. Mechoso, 2003: Parameterization of cloud-radiation processes in the UCLA general circulation model. *J. Climate*, **16**, 3357–3370.
- Lacis, A., and V. Oinas, 1991: A description of the correlated k-distribution method for modeling nongray gaseous absorption, thermal emission, and multiple scattering in vertically inhomogeneous atmospheres. *J. Geophys. Res.*, **96**, 9027–9063.
- Liou, K. N., 2002: *An Introduction to Atmospheric Radiation*. 2nd ed., Academic Press, 583pp.
- McClatchey, R. A., R. W. Fenn, J. E. A. Selby, F. E. Volz, and J. S. Garing, 1971: Optical properties of the atmosphere. Rep. AFCRL-71-0279, Air Force Cambridge Res. Lab., Bedford, MA, 85pp.
- McClatchey, R. A., W. S. Benedict, S. A. Clough, D. E. Burch, R. F. Calfee, K. Fox, C. S. Rothman, and

- J. S. Garing, 1973: AFCRL atmospheric absorption line parameters compilation. Environ. Res. Air Force Cambridge Res. Lab., Hanscom AFB, Bedford, MA. 434pp.
- Mlawer, E. J., S. J. Taubman, P. D. Brown, M. J. Iacono, and S. A. Clough, 1997: Radiative transfer for inhomogeneous atmospheres: RRTM, a validated correlated-k model for the longwave. *J. Geophys. Res.*, **102**, 16,663–16,682.
- Shi, G. Y., 1998: On the k-distribution and correlated k-distribution models in the atmospheric radiation calculation. *Scientia Atmospherica Sinica*, **22**(4), 659–676.
- Wang, W. C., and P. B. Ryan, 1983: Overlapping effect of atmospheric H₂O, CO₂ and O₃ on the CO₂ radiative effect. *Tellus B*, **35**, 81–91.